Received: 14 November 2019 | Revised: 29 January 2021 | Accepted: 23 February 2021

DOI: 10.1002/zamm.201900313

ORIGINAL PAPER

First yield in the Maugis-adhesive contact of elastic spheres

Jean-Emmanuel Leroy | **Emanuel Willert**

Technische Universität Berlin, Berlin 10623, Germany

Correspondence
Jean-Emmanuel Leroy, Technische Universität Berlin, Straße des 17. Juni 135, 10623 Berlin, Germany.
Email: leroy@campus.tu-berlin.de

We analyze the onset of plastic yield in the Maugis-adhesive contact of elastic spheres. Written in proper dimensionless variables, the problem solution depends on Poisson's ratio, the Tabor parameter and a non-dimensional adhesion strength. The influences of adhesion range and strength are studied in detail. First yield can either occur inside the bodies on the axis of symmetry (for long range adhesion) or at the contact boundary (for short range adhesion). Adhesion significantly reduces the external load necessary to initiate plastic yield. A simple analytic solution for the critical load in the DMT-limit of adhesion is being derived. Our results are quantitatively similar to previously published findings based on the double Hertz model of adhesion and can for example be applied to study an adhesive spherical microcontact in the contact of rough surfaces.

KEYWORDS
adhesion, first yield, Maugis theory, von Mises criterion

1 | INTRODUCTION

Contacts are highly stressed components of structures. By examining the state of stress inside the contacting bodies, it is possible to determine the contact load to locally initiate plastic yield. In Hertzian contact, for example, this problem has been solved long ago.

The influence of adhesion on plastic yield is high due to the stress concentration at the edge of adhesive contacts, which can be thought of as an "external crack". Yet, the interplay of adhesion and plasticity is still poorly understood.

Mesarovic and Johnson [1] investigated the influence of plasticity on the decohesion behavior of adhesive spheres. They assumed that one can neglect the influence of the adhesion during the elastoplastic loading, and that restitution, as in the non-adhesive case, is an elastic process. A similar model was later proposed by Olsson and Larsson [2]. Kogut and Etsion [3] developed a FE-model of an adhesive elastoplastic microcontact in the DMT limit [4] of adhesion. FE simulations with a Lennard-Jones model for the adhesive potential were done by Du et al. [5] and Kadin et al. [6]. Gilabert et al. [7] performed MD simulations for the JKR-adhesive [8] contact between an elastoplastic sphere and a rigid flat.

Due to their constitutive non-linearity, elastoplastic contact simulations are numerically costly. We will therefore focus on the problem of first yield in adhesive contacts. In the JKR limit of adhesive interaction, the stresses at the contact edge are singular. Hence, at an arbitrarily small load, there would be plastic deformation in a finite environment of the contact boundary. In the opposite DMT limit of adhesion the contact pressure distribution is the same as in the non-adhesive case with a reduced normal force; first yield thus occurs on the axis of symmetry at a lower load than in the non-adhesive contact.

Both limiting cases are insufficient to investigate the problem; in fact, the stress concentration at the contact boundary is finite, so a reasonable framework for solving the problem must take into account the Tabor parameter [9] for characterizing

the range of adhesion. In the work of Wu and Adams [10], the authors used the double Hertz model by Greenwood and Johnson [11] for the adhesive potential to analyze first yield in the adhesive contact of elastic spheres. The double Hertz model has some physically strange properties, but simplifies the contact mechanics of the problem as much as possible. An alternative approach to be pursued in the present paper is to use the solution of the adhesive normal contact problem with arbitrary range of adhesion according to Maugis [12], based on the Dugdale model [13] for the adhesive interaction.

The present paper is organized as follows: First, we will detail the theoretical foundations and associated numerical methods regarding the Maugis-adhesive contact of elastic spheres and the onset of plastic yield. Then, comprehensive results for the compressive normal force necessary to initiate plastic deformations, and for the exact location of first yield will be presented. Some conclusive remarks finish the manuscript.

2 | PROBLEM FORMULATION AND METHODS

2.1 | Maugis-adhesive contact of elastic spheres

Maugis obtained a solution for the adhesive contact of elastic spheres with variable range of adhesion by analogy to an external axisymmetric crack under pressure. According to the Dugdale model, the adhesive stress σ_0 is constant from the radius a of the crack to the radius c, where the distance between the surfaces is equal to the critical value

$$h = \frac{w}{\sigma_0}, \tag{1}$$

w being the work of adhesion. Beyond this radius no attraction forces remain.

Using results of Lowengrub and Sneddon [14] to calculate elastic displacements of the crack lips and the distribution of stresses, and considering the Griffith criterion [15], which equates the energy release rate to the work of adhesion, Maugis derived the set of equations

$$\text{I: } 0 = \frac{\lambda\bar{a}^2}{2}\left(\left(m^2-2\right)\arccos\left(\frac{1}{m}\right)+\sqrt{m^2-1}\right)+\frac{4\lambda^2\bar{a}}{3}\left(\sqrt{m^2-1}\arccos\left(\frac{1}{m}\right)-m+1\right)-1, \tag{2}$$

$$\text{II: } 0 = \bar{a}^3-\lambda\bar{a}^2\left(\sqrt{m^2-1}+m^2\arccos\left(\frac{1}{m}\right)\right)-\bar{P}, \tag{3}$$

$$\text{III: } 0 = \bar{a}^2-\frac{4}{3}\lambda\bar{a}\sqrt{m^2-1}-\bar{d}, \tag{4}$$

with the dimensionless parameters

$$\bar{a} = \frac{a}{\left(\frac{w\pi R^2}{K}\right)^{\frac{1}{3}}},\quad \bar{P} = \frac{P}{w\pi R},\quad \bar{d} = \frac{d}{\left(\frac{\pi^2 w^2 R}{K^2}\right)^{\frac{1}{3}}},\quad \lambda = \frac{2\sigma_0}{\left(\frac{\pi w K^2}{R}\right)^{\frac{1}{3}}} \text{ and } m = \frac{c}{a}, \tag{5}$$

where P is the applied contact load, a the radius of contact, c the outer radius of adhesion, d the indentation depth, $R = (1/R_1 + 1/R_2)^{-1}$ the reduced radius of the spheres and $K = 4/3 \cdot ((1-\nu_1^2)/E_1 + (1-\nu_2^2)/E_2)^{-1}$ the combined stiffness of the spheres, ν being the Poisson's ratio and E the Young modulus. The parameter λ determines the range of adhesion and is therefore proportional to the one proposed by Tabor. For $\lambda \to \infty$ the JKR limit is reached, while $\lambda \to 0$ leads to the DMT limit.

When specifying λ as well as the contact load $\bar{P}$, Equations (2) and (3) give the radius of contact $\bar{a}$ and the ratio of radii m. Those can be inserted in Equation (4) to calculate the indentation depth $\bar{d}$. Since there is no analytical solution for Equations (2) and (3), the Levenberg-Marquardt algorithm [16,17] was used to minimize the expression

$$F(\bar{a}, m) = \frac{1}{2}\sum_{i=1}^{2}\left[f_i(\bar{a}, m)\right]^2, \tag{6}$$

with f_i being the right sides of Equations (2) and (3), and thus obtain a numerical solution of the equation system. Once the radius of contact $\bar{a}$ and the ratio of radii m are determined through the set of equations, the pressure distribution of the Maugis-adhesive contact is given in dimensionless form with

$$\bar{p}(\bar{r}) = \begin{cases} \frac{3\bar{a}}{\pi}\sqrt{1-\bar{r}^2} - \frac{2\lambda}{\pi}\arctan\left(\frac{\sqrt{m^2-1}}{\sqrt{1-\bar{r}^2}}\right), & r \le a, \\ -\lambda, & a < r \le c, \\ 0, & c < r, \end{cases} \tag{7}$$

where the pressure is normalized in the same way as the adhesive stress

$$\bar{p} = \frac{2p}{\left(\frac{\pi w K^2}{R}\right)^{\frac{1}{3}}} \tag{8}$$

and $\bar{r} = r/a$.

2.2 | First yield

To determine the point of first yield, the stresses within the elastic half-space induced by the applied pressure distribution of Maugis need to be computed. These can be obtained by superposition of the stresses caused by a concentrated normal load (originally found by Boussinesq [18] and also given, e.g., by Johnson [19]), that is, integration over the whole pressure distribution.

Since the entire problem is axisymmetric, the same applies for the stresses in the elastic half-space and we use cylindrical coordinates. This also implies that the stresses $\sigma_{r\phi}$ and $\sigma_{\varphi z}$ are always equal to zero. The stress in the direction rr for instance is calculated through:

$$\sigma_{rr} = \int_0^c \int_0^{2\pi} \frac{p(r)}{2\pi}\left(\frac{1-2\nu}{s^2}\left(\left(1-\frac{z}{t}\right)\frac{x^2-y^2}{s^2} + \frac{zy^2}{t^3}\right) - \frac{3zx^2}{t^5}\right) r \mathrm{d}\varphi \mathrm{d}r, \tag{9}$$

where $s^2 = x^2 + y^2$, $t^2 = x^2 + y^2 + z^2$ and

$$x = r' - r\cos(\varphi),\ y = -r\sin(\varphi)\ \text{ and }\ z = z' \tag{10}$$

are the distances between the point (r', z') within the half-space and a point (r, φ) of the pressure distribution. Normalized to the yield strength of the softer material, σ_Y, Equation (9) can be written in dimensionless form:

$$\bar{\sigma}_{rr}(\bar{r}', \bar{z}') = \frac{\sigma_{rr}}{\sigma_\mathrm{Y}} = \frac{\psi}{2\pi}\int_0^m \int_0^{2\pi} \bar{p}(\bar{r})\left(\frac{1-2\nu}{\bar{s}^2}\left(\left(1-\frac{\bar{z}}{\bar{t}}\right)\frac{\bar{x}^2-\bar{y}^2}{\bar{s}^2} + \frac{\bar{z}\bar{y}^2}{\bar{t}^3}\right) - \frac{3\bar{z}\bar{x}^2}{\bar{t}^5}\right) \bar{r}\mathrm{d}\varphi\mathrm{d}\bar{r}, \tag{11}$$

where all lengths have been normalized to the radius of contact a. The parameter

$$\psi^3 = \frac{\pi w K^2}{8R\sigma_\mathrm{Y}^3} \tag{12}$$

contains the ratio of the critical load in the JKR model and the load leading to yielding in the Hertzian contact, and therefore can be thought of as a parameter scaling the adhesion strength. The integrals which need to be solved in order to obtain the stresses—for instance, the ones in Equation (11)—do not have an analytical solution for a pressure distribution from a Maugis-adhesive contact. We hence used the MATLAB function `integral2` [20], which is based on an adaptive 2D Gaussian quadrature, to calculate the integrals. It is noteworthy that a solution was only found for points

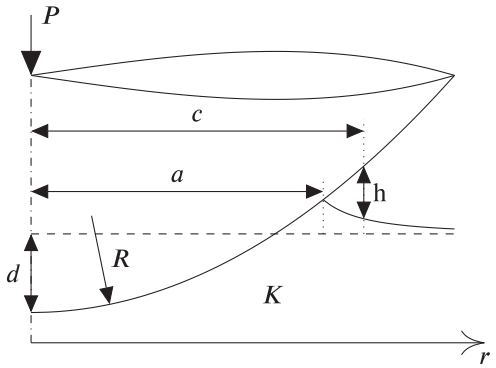

FIGURE 1 Maugis-adhesive contact between a rigid sphere with radius R and an elastic half-space with stiffness K

$\bar{z}' \geq 10^{-7}$; below this value, the gradients of the functions to integrate are getting too large to obtain an accurate numerical approximation.

To predict the onset of plastic yield within the elastic half-space, the von Mises yield criterion was used. The von Mises stress is the second invariant of the deviatoric stress tensor:

$$\sigma_{\mathrm{vM}} = \sqrt{\frac{1}{2}\Big(\left(\sigma_{rr} - \sigma_{\varphi\varphi}\right)^2 + \left(\sigma_{\varphi\varphi} - \sigma_{zz}\right)^2 + \left(\sigma_{zz} - \sigma_{rr}\right)^2 + 6\left(\sigma_{r\varphi}^2 + \sigma_{\varphi z}^2 + \sigma_{rz}^2\right)\Big)}, \tag{13}$$

and yielding occurs if $\sigma_{\mathrm{vM}} \geq \sigma_{\mathrm{Y}}$. Since the stress tensor and therefore the von Mises stress can be calculated in every point of the elastic half-space, but cannot be expressed as an analytical function of the coordinates r and z, search algorithms were used to determine its maximum value within the half-space. For the search on the axis of symmetry (in one dimension, z) the golden-section search introduced by Kiefer [21] was applied, while the maximum away from the axis of symmetry (a search in two dimensions, r and z) was determined using the Nelder-Mead method [22].

For the Hertzian non-adhesive problem, the onset of yield can be determined analytically and always occurs on the axis of symmetry. Johnson [19] states that for a Poisson's ratio of $\nu = 0.3$ yielding starts at a depth of $z = 0.48a$ in the half-space, when the mean pressure is equal to

$$\frac{P}{\pi a^2} = \frac{16}{15}\sigma_{\mathrm{Y}}. \tag{14}$$

An analysis of the stresses within the elastic half-space shows, however, that this is a rounded value. The more accurate value is $1.0752\ \sigma_{\mathrm{Y}}$, which leads to a yield load of

$$P_{\mathrm{Y}}^{(\mathrm{Hertz})} = 38.5403\frac{R^2\sigma_{\mathrm{Y}}^3}{K^2}. \tag{15}$$

3 | RESULTS

There are two locations in the elastic half-space, where yielding might start. These can be seen in Figure 2, which shows the stress distribution within the half-space for a mid-range Tabor parameter of $\lambda = 3$. Local maxima are visible in two points within this stress field. They resemble the global maxima of the respective limiting theories: Just like for the DMT limit (producing a Hertzian stress field), there is a maximum on the axis of symmetry rather far away from the half-space boundary; and similar to the JKR limit (with a singularity in stress at the edge of contact), there is a maximum close to the half-space boundary and the edge of contact. Depending on the Tabor parameter and the applied contact force, these two local maxima are pronounced to a greater or lesser extent. In the presented figure, for instance, at a load of $\bar{P} = 39.98$ and an adhesion parameter of $\psi = 0.4836$, yield is starting simultaneously on the axis of symmetry and at the edge of contact.

For better legibility of the results obtained, we now introduce the new dimensionless force

$$P^* = \bar{P}\psi^3 = \frac{P}{8\dfrac{R^2\sigma_{\mathrm{Y}}^3}{K^2}}, \tag{16}$$

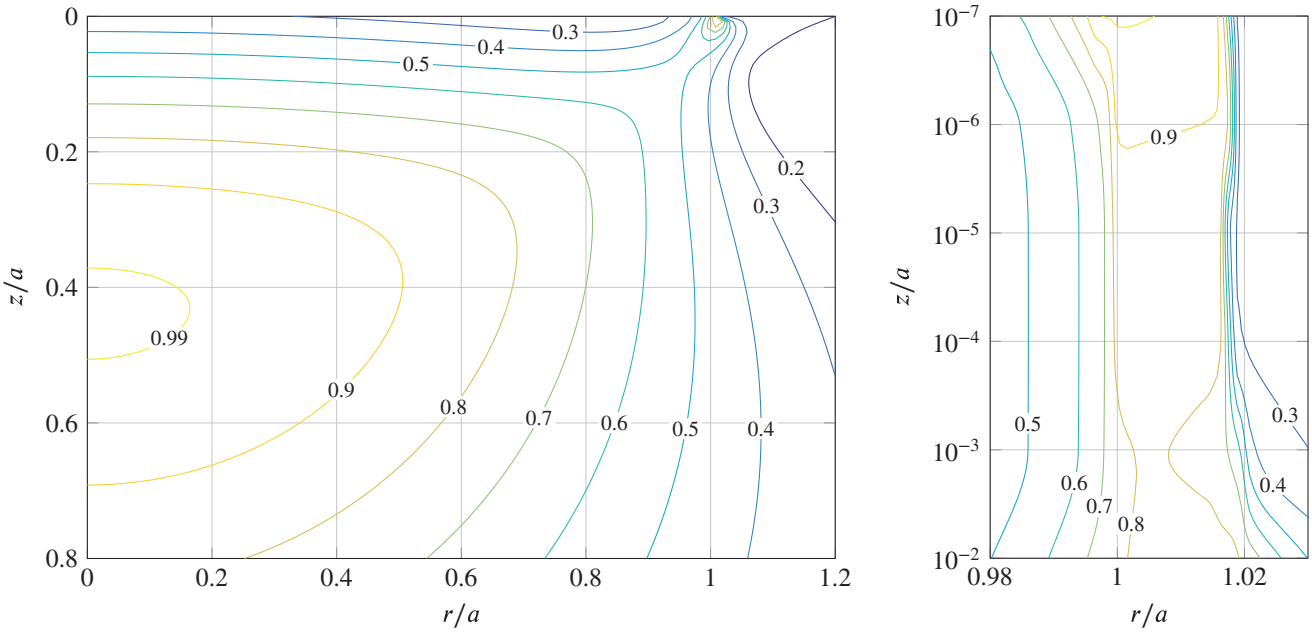

(a) Overall view of the elastic half-space.

(b) Detailed view of the edge of contact.

FIGURE 2 Distribution of the normalized von Mises stress $\sigma_{\mathrm{vM}}/\sigma_{\mathrm{Y}}$ for a Maugis-adhesive contact with $\lambda = 3$, $\psi = 0.4836$, $\bar{P} = 39.98$ and $\nu = 0.3$, which represents the point where yielding occurs simultaneously on the axis of symmetry and at the edge of contact

which corresponds to a normalization to the yield load from the Hertzian contact. The results are presented in dependency on the two main parameters λ and ψ, i. e. the range and the strength of adhesion. The third parameter, the Poisson's ratio ν, was set to 0.3 throughout all calculations.

3.1 | The DMT limit

Once the dimensionless force P^* is introduced, the yield load for the DMT limit ($\lambda \to 0$) can easily be expressed as a function of the adhesion parameter ψ. It differs from the Hertzian yield load by the adhesion force between two rigid spheres after Bradley [23]:

$$P_{\mathrm{Y}}^{(\mathrm{DMT})} = P_{\mathrm{Y}}^{(\mathrm{Hertz})} - 2w\pi R, \tag{17}$$

which leads to the dimensionless form

$$P_{\mathrm{Y}}^{*(\mathrm{DMT})} = P_{\mathrm{Y}}^{*(\mathrm{Hertz})} - 2\psi^3. \tag{18}$$

3.2 | Normal force to initiate yield

For a variable range of adhesion the computed yield loads are shown in Figures 3 and 4. The solid lines are for yielding on the axis of symmetry, while yielding near the edge of contact is represented by dashed lines. These are not present in Figure 4, since for values below $\lambda = 1.236$ and loads greater than zero the onset of yield always occurs on the axis of symmetry.

If considering yield on the axis of symmetry only (and neglecting plastic deformation at the edge of contact), results are similar for all ranges of adhesion: For values of the adhesion parameter ψ going towards zero, the yield force approaches the one predicted by the Hertzian theory, that is, $P_{\mathrm{Y}}^{*(\mathrm{Hertz})} = 4.8175$. With ψ getting higher, entailing a greater influence of adhesion, the yield force gradually decreases until yielding occurs with no applied load for a certain value of the adhesion

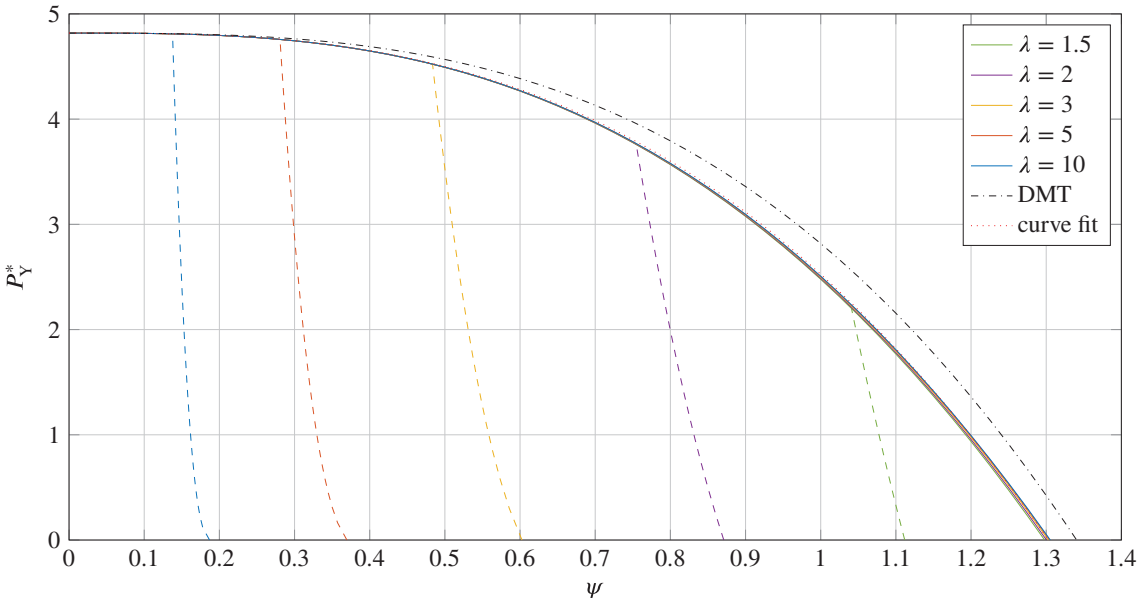

FIGURE 3 Normal force for the initiation of yield over the adhesion parameter ψ for different ranges of adhesion λ. Results are displayed for yielding on the axis of symmetry (solid lines) and yielding near the contact edge (dashed lines) as well as curves for the DMT limit and the proposed analytical fit

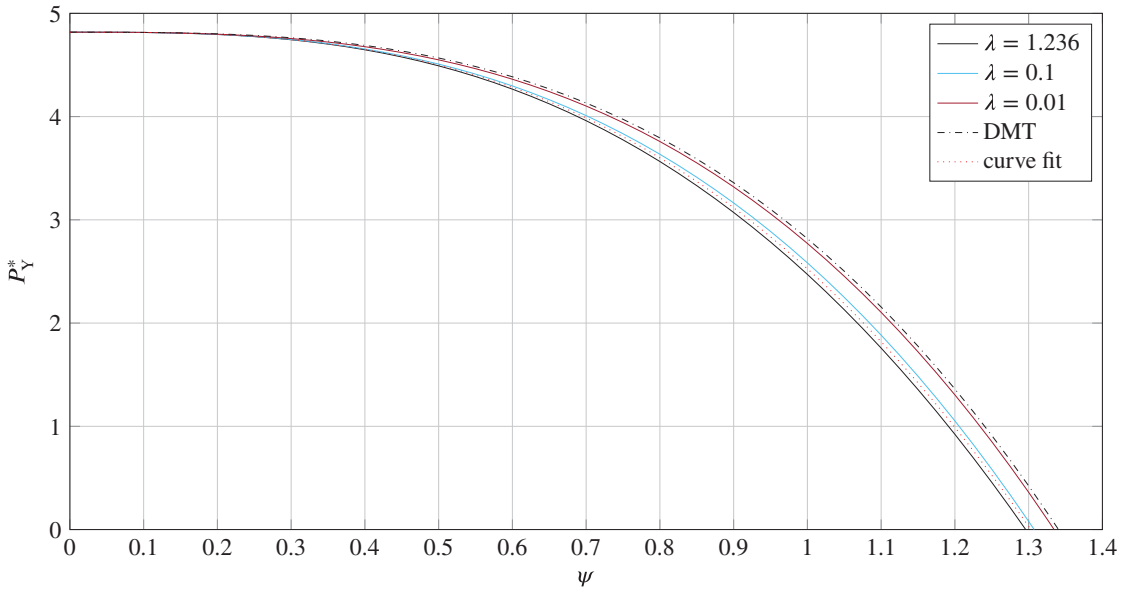

FIGURE 4 Normal force for the initiation of yield over the adhesion parameter ψ for further ranges of adhesion λ (yielding on the axis of symmetry only). Curves for the DMT limit and the proposed analytical fit can be seen as well

parameter. We present the following curve fit expression

$$P^*_{\mathrm{Y(fit)}} = 0.2838\psi^4 - 2.4454\psi^3 - 0.1426\psi^2 + 0.0122\psi + 4.8175 \tag{19}$$

which is suited to describe the onset of yield on the axis of symmetry for values of λ in the range $[0.1; 10]$.

Table 1 shows exemplary values for the parameter ψ for contacts between equal materials.[1] While the contacts of both metals presented are described by values for ψ that are situated well inside the range where yield occurs instantly at no

[1] Elastic and mechanical properties were taken from [24] and [25], surface energies (i.e., half the work of adhesion for contacts between equal materials) from [26] and [27].

TABLE 1 Parameter ψ for different materials and radii

Material	Combined stiffness K (GPa)	Yield strength σ_Y (MPa)	Work of adhesion w (mJ/m^2)	Parameter ψ for $R = 1\mu$m	Parameter ψ for $R = 10\mu$m
Aluminium alloy	53	95	88	4.84	2.25
Mild steel	147	250	114	3.96	1.84
Polyethylen	0.3	20	66	0.66	0.31
PMMA	2.3	62	106	0.97	0.45

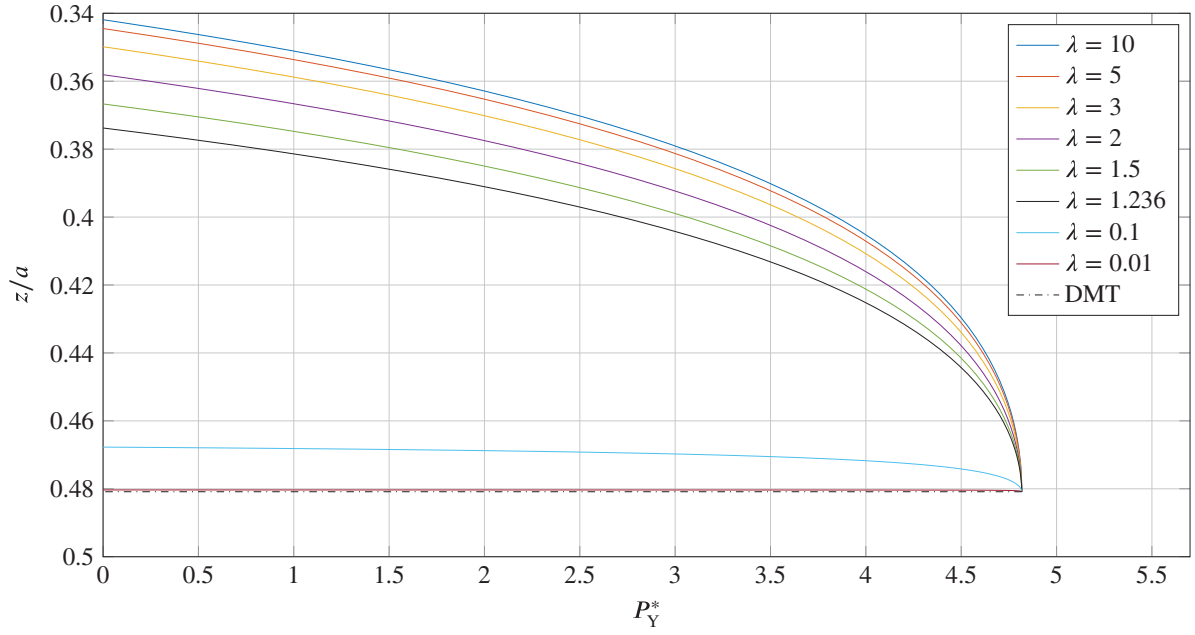

FIGURE 5 Point of first yield on the axis of symmetry over the critical force to cause yielding for different ranges of adhesion λ

applied load, for the contacts between polymers the values for ψ lie within the range of results presented for positive yield forces.

When taking into consideration yielding in the entire half-space, starting from $\psi = 0$, the onset of yield still takes place first on the axis of symmetry, but then suddenly jumps to the edge of contact (where the crossing of solid and dashed lines represents yielding in the two locations simultaneously). After that yield loads are rapidly falling for increasing ψ. Moreover, the value of the adhesion parameter for jumping from the axis of symmetry to the edge of contact is strongly depending on the range of adhesion. This dependency was to expect, since within the pressure distribution from Equation (7) the negative pressure at the radius of contact is equal to λ and therefore directly linked to the Tabor parameter and thus the range of adhesion.

3.3 | Point of first yield

The point where yielding occurs for the first time on the axis of symmetry (that is the z-axis) is plotted against the force required to initiate this yielding in Figure 5. For all ranges of adhesion the limit $\psi \to 0$ and consequently a yield load $\bar{P}_Y$ going towards infinity lead to the first yield occurring at the same point $z = 0.4809a$ as in the Hertzian theory and thus the DMT limit. But starting from the Hertzian value $P_Y^{*(\text{Hertz})} = 4.8175$, as the yield load decreases, the point of first yield moves towards the half-space boundary. The higher the Tabor parameter λ, and therefore the smaller the range of adhesion, the more the point of first yield shifts upwards on the axis of symmetry for small contact loads. Interestingly enough, detailed analysis of the stresses within the half-space shows, that for yielding occurring at smaller values of z (that is high Tabor parameters and small contact loads) the hydrostatic pressure in the point of first yield is significantly lower compared to the Hertzian theory.

As far as the onset of yield at the edge of contact is concerned, the applied search algorithm did always converge to the point $(\bar{r}, \bar{z}) = (1, 10^{-7})$. It is to note that $\bar{z} = 10^{-7}$ was set as a limit, since for smaller values integrals within the calculation of stresses could no longer be solved. It is plausible, therefore, that the point of first yield is located on the boundary of the half-space at $(\bar{r}, \bar{z}) = (1, 0)$, just like in the JKR theory.

4 | DISCUSSION

The results displayed above which have been obtained based on the Dugdale-Maugis description of adhesive contact are quantitatively similar to those presented by Wu and Adams for the double Hertz model of adhesive contact by Greenwood and Johnson. This seems to suggest that the precise form of the adhesive potential is of lesser importance for the onset of plastic yield in the adhesive contact of elastic spheres.

To determine the contact configuration at first yield, we only applied the shear strain-energy criterion by von Mises. Hence, all our results are obviously only applicable for materials whose mechanisms to release inelastic stresses are captured by this yield criterion. For example, this is probably not the case for the wide class of adhesive contacts formed by very soft (and often viscoelastic) biomaterials. Also note that it has been shown in Finite-Element simulations that, especially for large indentation depths, there are differences in elastoplastic contacts between indentation (i.e., contact between a rigid sphere and a deformable flat) and flattening problems (where instead the sphere is deformable). This aspect, which has not been captured in our analysis, is detailed in the review by Ghaednia et al. [28].

We also did not consider effects of interface friction (which may be important in the case of elastically dissimilar materials) or surface roughness. The interplay of friction, roughness and adhesion is a vast topic of ongoing scientific research, that Ciavarella et al. [29] gave a deep and comprehensive review for. Moreover, several recent works have dealt with the interplay of friction and adhesion—especially shear-induced reduction of the contact area and adhesive forces for soft materials—from the perspective of Linear Elastic Fracture Mechanics (LEFM), that is, the framework we are working in using the Dugdale-Maugis model. Papangelo and Ciavarella [30] demonstrated the sensitivity of the problem to the concrete superposition functions of different crack modes ([31], [32]). Also, it has been shown [33] that, of the two main assumptions of the LEFM treatment of frictional adhesion—namely the singularity of shear stresses and the absence of dissipation in the contact—only the second plays a relevant role for the physical description. Lengiewicz et al. [34] successfully attributed the shear-induced contact area reduction in soft elastic materials to contact lifting due to finite deformations and non-linear elasticity. However, our results could be used to analyze an adhesive microcontact in more detail. For example, Das and Chasiotis [35] recently demonstrated that the Dugdale-Maugis model, together with LEFM, can predict the tangential pull-off force instabilities obtained in experiments for adhesive nanoscale polymer contacts.

5 | CONCLUSIONS

Based on the Dugdale-Maugis model of adhesive contact and the von Mises stress criterion, we studied the influence of adhesion strength and adhesion range on the onset of plastic yield in the adhesive contact of elastic spheres theoretically. We find that yield can be first initiated either on the axis of symmetry inside the softer sphere (for small values of the Tabor parameter, i.e., long range adhesion) or at the contact boundary (for large values of the Tabor parameter). In both cases adhesion severely reduces the external load necessary to initiate plastic yield. For yielding on the axis of symmetry the Tabor parameter has almost no influence on the critical load and the simple analytical solution for the DMT-limit can be used. Nevertheless, in this case, the point of first yield moves towards the surface for stronger adhesion and the hydrostatic component of the stress state is reduced.

The results obtained are quantitatively similar to previously published findings based on the double Hertz model of adhesion. This suggests that the precise form of the adhesive potential has only a small influence on the onset of plastic yield.

ACKNOWLEDGEMENTS

We acknowledge support by the German Research Foundation and the Open Access Publication Fund of TU Berlin.

Open access funding enabled and organized by Projekt DEAL.

CONFLICT OF INTEREST

The authors declare no potential conflict of interests.

AUTHOR CONTRIBUTIONS

Emanuel Willert provided analytical results, Jean-Emmanuel Leroy performed the numerical calculations. The manuscript was prepared by both authors.

ORCID

Jean-Emmanuel Leroy https://orcid.org/0000-0002-2587-3962
Emanuel Willert https://orcid.org/0000-0001-7535-7301

REFERENCES

[1] Mesarovic, S.D., Johnson, K.L.: Adhesive contact of elastic-plastic spheres. J. Mech. Phys. Solids 48(10), 2009–2033 (2000)
[2] Olsson, E., Larsson, P.L.: On force-displacement relations at contact between elastic-plastic adhesive bodies. J. Mech. Phys. Solids 61(5), 1185–1201 (2013)
[3] Kogut, L., Etsion, I.: Adhesion in elastic-plastic spherical microcontact. J. Colloid Interface Sci. 261(2), 372–378 (2003)
[4] Derjaguin, B.V., Muller, V.M., Toporov, Y.P.: Effect of contact deformations on the adhesion of particles. J. Colloid Interface Sci. 53(2), 314–326 (1975)
[5] Du, Y., et al.: A finite element model of loading and unloading of an asperity contact with adhesion and plasticity. J. Colloid Interface Sci. 312(2), 522–528 (2007)
[6] Kadin, Y., Kligerman, Y., Etsion, I.: Loading-unloading of an elastic-plastic adhesive spherical microcontact. J. Colloid Interface Sci. 321(1), 242–250 (2008)
[7] Gilabert, F.A., Quintanilla, M.A.S., Castellanos, A., Valverde, J.M.: Adhesive elastic plastic contact: theory and numerical simulation. ZAMM Z. Angew. Math. Mech. 87(2), 128–138 (2007)
[8] Johnson, K.L., Kendall, K., Roberts, A.D.: Surface energy and the contact of elastic solids. Proc. R. Soc. Lond. A 324, 301–313 (1971)
[9] Tabor, D.: Surface forces and surface interactions. J. Colloid Interface Sci. 58(1), 2–13 (1977)
[10] Wu, Y.C., Adams, G.G.: Plastic yield conditions for adhesive contacts between a rigid sphere and an elastic half-space. J. Tribol. 131(1), 011403–1–011403–7 (2008)
[11] Greenwood, J.A., Johnson, K.L.: An alternative to the Maugis model of adhesion between elastic spheres. J. Phys. D: Appl. Phys. 31(22), 3279–3290 (1998)
[12] Maugis, D.: Adhesion of spheres: the JKR-DMT transition using a Dugdale model. J. Colloid Interface Sci. 150(1), 243–269 (1992)
[13] Dugdale, D.S.: Yielding of steel sheets containing slits. J. Mech. Phys. Solids 8(2), 100–104 (1960)
[14] Lowengrub, M., Sneddon, I.N.: The distribution of stress in the vicinity of an external crack in an infinite elastic solid. Int. J. Eng. Sci. 3(4), 451–460 (1965)
[15] Griffith, A.: The phenomena of rupture and flow in solids. Philos. Trans. R. Soc. London A 221(582-593), 163–198 (1921)
[16] Marquardt, D.: An algorithm for least-squares estimation of nonlinear parameters. J. Soc. Ind. Appl. Math. 11(2), 431–441 (1963)
[17] Levenberg, K.: A method for the solution of certain non-linear problems in least squares. Q. Appl. Math. 2(2), 164–168 (1944)
[18] Boussinesq, J.: Application des potentiels à l'étude de l'équilibre et du mouvement des solides élastiques: principalement au calcul des déformations et des pressions que produisent, dans ces solides, des efforts quelconques exercés sur une petite partie de leur surface ou de leur intérieur: mémoire suivi de notes étendues sur divers points de physique, mathematique et d'analyse, vol. 4. Gauthier-Villars (1885)
[19] Johnson, K.: Contact Mechanics. Cambridge University Press (1987)
[20] Shampine, L.: Matlab program for quadrature in 2D. Appl. Math. Comput. 202(1), 266–274 (2008)
[21] Kiefer, J.: Sequential minimax search for a maximum. Proc. Am. Math. Soc. 4(3), 502–506 (1953)
[22] Nelder, J., Mead, R.: A simplex method for function minimization. Compu. J. 7(4), 308–313 (1965)
[23] Bradley, R.: The cohesive force between solid surfaces and the surface energy of solids. Philos. Mag. 13(86), 853–862 (1932)
[24] Gale, W., Totemeier, T. (eds.): Smithells Metals Reference Book. Elsevier (2003)
[25] Brinson, H., Brinson, L.: Characteristics, applications and properties of polymers. In: Polymer Engineering Science and Viscoelasticity, pp. 57–100. Springer (2015)
[26] Harris, A., Beevers, A.: The effects of grit-blasting on surface properties for adhesion. Int. J. Adhesion Adhesives 19(6), 445–452 (1999)
[27] Mangipudi, V., Falsafi, A.: Direct estimation of the adhesion of solid polymers. In: Dillard, D., Pocius, A., Chaudhury, M. (eds.) Adhesion Science and Engineering, pp. 75–138. Elsevier (2002)
[28] Ghaednia, H., Wang, X., Saha, S., Xu, Y., Sharma, A., Jackson, R.L.: A review of elastic-plastic contact mechanics. Appl. Mech. Rev. 69(6), 060804–1–060804–30 (2017)
[29] Ciavarella, M., Joe, J., Papangelo, A., Barber, J.R.: The role of adhesion in contact mechanics. J. R. Soc. Interface 16(151), 20180738–1–20180738–22 (2019)
[30] Papangelo, A., Ciavarella, M.: On mixed-mode fracture mechanics models for contact area reduction under shear load in soft materials. J. Mech. Phys. Solids 124, 159–171 (2019)
[31] Hutchinson, J.W., Suo, Z.: Mixed mode cracking in layered materials. Adv. Appl. Mech. 29, 63–191 (1991)

[32] Johnson, K.L.: Adhesion and friction between a smooth elastic spherical asperity and a plane surface. Proc. R. Soc. Lond. A 453, 163–179 (1997)
[33] Ciavarella, M., Papangelo, A.: On the degree of irreversibility of friction in sheared soft adhesive contacts. Tribol. Lett. 68(81), (2020) s
[34] Lengiewicz, J., de Souza, M., Lahmar, M.A., Courbon, C., Dalmas, S., Stupkiewicz, D., Scheibert, J.: Finite deformations govern the anisotropic shear-induced area reduction of soft elastic contacts. J. Mech. Phys. Solids 143(104056), (2020)
[35] Das, D., Chasiotis, I.: Sliding of adhesive nanoscale polymer contacts. J. Mech. Phys. Solids 14(103931), (2020)

How to cite this article: Leroy J-E, Willert E. First yield in the Maugis-adhesive contact of elastic spheres. *Z Angew Math Mech*. 2021;e201900313. https://doi.org/10.1002/zamm.201900313